PROCEEDINGS OF SCIENCE

Oscillons and oscillating kinks in the Abelian-Higgs model

Charilaos Tsagkarakis*
Department of Physics, University of Athens
E-mail: ctsagkarakis@phys.uoa.gr

V. Achilleos
Department of Physics, University of Athens
E-mail: vachill@phys.uoa.gr.

F.K. Diakonos
Department of Physics, University of Athens
E-mail: fdiakono@phys.uoa.gr

D.J. Frantzeskakis
Department of Physics, University of Athens
E-mail: dfrantz@phys.uoa.gr

G.C. Katsimiga
Department of Physics, University of Athens
E-mail: liakatsim@gmail.com

X.N. Maintas
Department of Physics, University of Athens
E-mail: xmaintas@phys.uoa.gr

E. Manousakis
Department of Physics, University of Athens
Department of Physics, Florida State University, Tallahassee, Florida, USA
E-mail: emanous@phys.uoa.gr

A. Tsapalis
Department of Physics, University of Athens
Hellenic Naval Academy, Greece
E-mail: tsapalis@snd.edu.gr

PoS(CORFU2014)122

PROCEEDINGS OF SCIENCE

We study the classical dynamics of the Abelian Higgs model employing an asymptotic multiscale expansion method, which uses the ratio of the Higgs to the gauge field amplitudes as a small parameter. We derive an effective nonlinear Schrödinger equation for the gauge field, and a linear equation for the scalar field containing the gauge field as a nonlinear source. This equation is used to predict the existence of oscillons and oscillating kinks for certain regimes of the ratio of the Higgs to the gauge field masses. Results of numerical simulations are found to be in very good agreement with the analytical findings, and show that the oscillons are robust, while kinks are unstable. It is also demonstrated that oscillons emerge spontaneously as a result of the onset of the modulational instability of plane wave solutions of the model. Connections of the obtained solutions with the phenomenology of superconductors is discussed.

Proceedings of the Corfu Summer Institute 2014
3-21 September 2014
Corfu, Greece

*Speaker.

PoS(CORFU2014)122

1. Introduction

Soliton solutions of field theoritical models play a significant role in the description of physical phenonena occuring in a wide class of systems ranging from high energy physics to cold atoms and granular media [1, 2, 3, 4, 5, 6, 7, 8, 9, 10, 11, 12, 13, 14, 15, 16, 17, 18, 19, 20, 21, 22, 23, 24, 25]. In particular classical solutions of the mean field Gor'kov - Eliashberg - Landau - Ginzburg theory are important for the phenomenology of superconductivity [26, 27, 28, 29] where the emerging effective field theory is the Abelian-Higgs model. Several solutions of the latter are found [30, 31, 32].

In the present work [33], we analyze the classical dynamics of the Abelian-Higgs model in $(1+1)$-dimensions by means of a multiscale expansion method [35]. We restrict our analysis on the case of small fluctuations of the condensate about its vacuum expectation value (vev). This is realized by choosing the amplitude of the Higgs field to be an order of magnitude smaller than that of the gauge field. In this limit the dynamics simplify considerably and it is found that the scalar field performs asymmetric oscillations around the classical vacuum. Such a scenario occurs naturally considering the model just after the symmetry breaking i.e. close to the critical point. Then the minimum of the scalar field potential is very flat and the asymmetric cubic term is strong leading to an asymmetric shape of the potential around it. However, results are also found in the case where the gauge and the scalar field amplitudes are of the same order [34]. This scenario corresponds to a strong breaking of the underlying gauge symmetry, which is far beyond the related critical point. In this case the minimum of the potential occurs at the bottom of a deep well, while the potential shape is almost symmetric around it since the quadratic term dominates.

Employing the method of multiple scales (see also Ref. [36]), the original nonlinear coupled field equations are reduced to an effective nonlinear Schrödinger (NLS) equation for the gauge field, and a linear equation for the Higgs field containing the gauge field as a source. These equations are analytically solved giving two types of localized solutions for the gauge field, namely in the form of oscillons and oscillating kinks. Subsequently, we numerically integrate the original equations of motion using, as initial conditions, the analytically found solutions. We find that the analytical predictions are in excellent agreement with the numerical findings for a large range of values of the parameters involved. We then discuss connections between the Abelian-Higgs model solutions and the phenomenology of superconducting materials, describing the temporal fluctuations of the condensate in a one-dimensional (1D) Josephson junction [37] due to the presence of oscillating (in time) magnetic and electric fields.

2. The model and its analytical consideration

2.1 Formulation and Equations of Motion

The $U(1)$-Higgs field dynamics is described by the Lagrangian:

$$\mathscr{L} = -\frac{1}{4}F_{\mu\nu}F^{\mu\nu} + (D_\mu\phi)^*(D^\mu\phi) - V(\Phi^*\Phi), \tag{2.1}$$

where $F_{\mu\nu}$ is the $U(1)$ field strength tensor, $D_\mu = \partial_\mu + ie\tilde{A}_\mu$ is the covariant derivative, and $V(\Phi^*\Phi) = \mu^2\Phi^*\Phi + \lambda(\Phi^*\Phi)^2$ ($\lambda > 0$) is the Higgs self-interaction potential (asterisk denotes

complex conjugate). In the broken phase, $\mu^2 < 0$, a vev $\tilde{\upsilon}/\sqrt{2}$ of the Higgs field arises classically: $\tilde{\upsilon}^2 = -\mu^2/\lambda$. We will focus on the dynamics of this system assuming that the Higgs field fluctuates slightly around its vev. In this case, we expand the field Φ as: $\Phi = \frac{1}{\sqrt{2}}(\tilde{\upsilon} + \tilde{H})$ and obtain the following equations of motion for $\tilde{A}_\mu$ and $\tilde{H}$:

$$(\widetilde{\Box} + m_A^2)\tilde{A}_\mu - \partial_\mu(\partial_\nu \tilde{A}^\nu) + 2e^2\tilde{\upsilon}\tilde{H}\tilde{A}_\mu + e^2\tilde{H}^2\tilde{A}_\mu = 0, \tag{2.2}$$

$$(\widetilde{\Box} + m_H^2)\tilde{H} + 3\lambda\tilde{\upsilon}\tilde{H}^2 + \lambda\tilde{H}^3 - e^2\tilde{A}_\mu\tilde{A}^\mu(\tilde{\upsilon} + \tilde{H}) = 0, \tag{2.3}$$

where $m_A^2 = e^2\tilde{\upsilon}^2$ and $m_H^2 = 2\lambda\tilde{\upsilon}^2$. We simplify Eqs. (2.2)-(2.3) choosing the field representation $\tilde{A}_0 = \tilde{A}_1 = \tilde{A}_3 = 0$, and $\tilde{A}_2 = \tilde{A} \neq 0$. Due to the fact that we are interested in 1D settings, the non vanishing $\tilde{A}_2$ field is a function solely of x and t. As a consequence, the Lorentz condition $\partial_\nu \tilde{A}^\nu = 0$ is trivially fulfilled and we are left with a coupled system of equations for the gauge field $\tilde{A}(x,t)$ and the Higgs field. Furthermore, we write Eqs. (2.2)-(2.3) in a dimensionless form by rescaling the fields as: $\tilde{A} \to (m_A/e)A$, $\tilde{H} \to (m_A/e)H$, and space-time coordinates as: $\tilde{x} \to x/m_A$ and $\tilde{t} \to t/m_A$. Thus we end up with the following equations of motion:

$$(\Box + 1)A + 2AH + H^2A = 0, \tag{2.4}$$

$$(\Box + q^2)H + \frac{1}{2}q^2H^3 + \frac{3}{2}q^2H^2 + HA^2 + A^2 = 0, \tag{2.5}$$

where parameter $q \equiv m_H/m_A$ is assumed to be of order $\mathscr{O}(1)$. The Hamiltonian corresponding to the above equations of motion is:

$$\mathscr{H} = \frac{1}{2}\left[(\partial_t A)^2 + (\partial_x A)^2 + (\partial_t H)^2 + (\partial_x H)^2\right] + V, \tag{2.6}$$

where indices denote partial derivatives with respect to x and t, and the potential V is given by:

$$V = \frac{q^2}{8}H^4 + \frac{q^2}{2}H^3 + \frac{q^2}{2}H^2 + \frac{1}{2}H^2A^2 + HA^2 + \frac{1}{2}A^2. \tag{2.7}$$

Notice that V exhibits a single minimum at $(A,H) = (0,0)$.

2.2 Multiscale expansion and the NLS equation

Considering a small fluctuating field H, we may employ a perturbation scheme, which uses a formal small parameter $0 < \varepsilon \ll 1$ defined by the ratio of the amplitude of the Higgs field to the amplitude of the gauge field, i.e., $\varepsilon \sim H/A$. In particular, we will employ a multiscale expansion method [35], assuming that the Higgs and gauge fields depend on the set of independent variables $x_0 = x$, $x_1 = \varepsilon x$, $x_2 = \varepsilon^2 x, \ldots$ and $t_0 = t$, $t_1 = \varepsilon t$, $t_2 = \varepsilon^2 t, \ldots$. Accordingly, the partial derivative operators are given (via the chain rule) by $\partial_x = \partial_{x_0} + \varepsilon\partial_{x_1} + \ldots$, $\partial_t = \partial_{t_0} + \varepsilon\partial_{t_1} + \ldots$. Furthermore, taking into regard that the fields should be expanded around the trivial solution of Eqs. (2.4)-(2.5), as well as $H \sim \varepsilon A$ as per our assumption, we introduce the following asymptotic expansions for A and H:

$$A = \varepsilon A^{(1)} + \varepsilon^2 A^{(2)} + \ldots, \tag{2.8}$$

$$H = \varepsilon^2 H^{(2)} + \varepsilon^3 H^{(3)} + \ldots, \tag{2.9}$$

where $A^{(j)}$ and $H^{(j)}$ ($j=0,1,\ldots$) denote the fields at the order $\mathscr{O}(\varepsilon^j)$. Substituting Eqs. (2.8)-(2.9) into Eqs. (2.4)-(2.5), and using the variables $x_0, x_1, \ldots, t_0, t_1, \ldots$, we obtain the following system of equations up to the third-order in the small parameter epsilon $\mathscr{O}(\varepsilon^3)$:

$$\mathscr{O}(\varepsilon) : (\Box_0 + 1)A^{(1)} = 0, \tag{2.10}$$

$$\mathscr{O}(\varepsilon^2) : (\Box_0 + 1)A^{(2)} + 2(\partial_{t_0}\partial_{t_1} - \partial_{x_0}\partial_{x_1})A^{(1)} = 0, \tag{2.11}$$

$$(\Box_0 + q^2)H^{(2)} + A^{(1)2} = 0, \tag{2.12}$$

$$\mathscr{O}(\varepsilon^3) : (\Box_0 + 1)A^{(3)} + 2(\partial_{t_0}\partial_{t_1} - \partial_{x_0}\partial_{x_1})A^{(2)} + \left(\Box_1 + 2\partial_{t_0}\partial_{t_2} - 2\partial_{x_0}\partial_{x_2} + 2H^{(2)}\right)A^{(1)} = 0. \tag{2.13}$$

The solution of Eq. (2.10) at the first order is:

$$A^{(1)} = u(x_1, x_2, \ldots, t_2, t_3 \ldots)e^{i\theta} + \text{c.c.}, \tag{2.14}$$

where u is an unknown function, "c.c." stands for complex conjugate, while $\theta = Kx - \Omega t$, and the frequency Ω and wavenumber K are connected through the dispersion relation $\Omega^2 = K^2 + 1$. The solvability condition for the second-order equation (2.11), is $(\partial_{t_0}\partial_{t_1} - \partial_{x_0}\partial_{x_1})A^{(1)} = 0$ [1]. which satisfied in the frame moving with the group velocity $\upsilon_g \equiv \partial\Omega/\partial K$, so that u depends only on the variable $\tilde{x}_1 = x_1 - \upsilon_g t_1$ and t_2. Then, the field $A^{(2)}$ is taken to be of the same functional form as $A^{(1)}$ [cf. Eq. (2.14)]. Taking into account the above results, Eq. (2.12) for the Higgs field becomes:

$$H^{(2)} = B\left(b|u|^2 + u^2 e^{-2it} + \text{c.c.}\right), \tag{2.15}$$

where $B = 1/(4-q^2)$ and $b = -2/Bq^2$; here, it is assumed that $q \neq 0$ and $q \neq 2$, as for these limiting values the field $H^{(2)}$ (which is assumed to be of $\mathscr{O}(1)$ for the perturbation expansion to be valid) becomes infinitely large. Finally, at the order $\mathscr{O}(\varepsilon^3)$, we first note that the second term vanishes in the frame moving with υ. Thus, the solvability condition (obtained —as before— by requiring that the secular part is zero) becomes: $\left(\Box_1 + 2\partial_{t_0}\partial_{t_2} - 2\partial_{x_0}\partial_{x_2} + 2H^{(2)}\right)A^{(1)} = 0$. In the following, for simplicity, we will consider the zero momentum case ($K = 0$); hence, $\upsilon_g = 0$, and also $\tilde{x}_1 = x_1$, i.e., the field A_1 is at rest. In this case, we derive the following NLS equation for the unknown function $u(x_1, t_2)$:

$$i\partial_{t_2}u + \frac{1}{2}\partial_{x_1}^2 u + s|u|^2 u = 0, \tag{2.16}$$

where the parameter s is given by

$$s = \frac{2}{q^2} + \frac{1}{q^2 - 4}. \tag{2.17}$$

The above NLS equation possesses exact localized solutions of two different types, depending on the sign of s: for $s > 0$, the solutions are sech-shaped solitons, while for $s < 0$ the solutions are tanh-shaped kinks. These solutions have been extensively studied in a variety of physical contexts including nonlinear optics [38], water waves [39], atomic Bose-Einstein condensates [25], and so

[1] The second term is "secular", i.e., is in resonance with the first term which becomes $\propto \theta\exp(i\theta)$, thus leading to blow-up of the solution for $t \to +\infty$.

on. Here, the type of solution, i.e., the sign of the nonlinear term in Eq. (2.16), depends solely on the parameter q.

In particular, for $q < 1.63$ and $q > 2$, we obtain $s > 0$ [attractive (focusing) nonlinearity] and the soliton solution of Eq. (2.16) has the form:

$$u = u_0 \mathrm{sech}\left(\sqrt{s} u_0 x_1\right) e^{-i\omega t_2}, \tag{2.18}$$

where u_0 is a free parameter [considered to be of order $\mathcal{O}(1)$] characterizing the amplitude of the soliton, while the soliton frequency is $\omega = -(1/2)u_0^2 s$. Accordingly, the approximate solutions of Eqs. (2.4)-(2.5) for A and H can be expressed in terms of the original variables x and t as follows:

$$A \approx 2\varepsilon u_0 \mathrm{sech}\left(\varepsilon u_0 \sqrt{s} x\right) \cos\left[\left(1 - \frac{1}{2}(\varepsilon u_0)^2 s\right) t\right], \tag{2.19}$$

$$H \approx (\varepsilon u_0)^2 B \mathrm{sech}^2\left(\varepsilon u_0 \sqrt{s} x\right) \left\{b + 2\cos\left[2\left(1 - \frac{1}{2}(\varepsilon u_0)^2 s\right) t\right]\right\}, \tag{2.20}$$

characterized by the single free parameter εu_0. The above approximate solutions for the gauge field A and the Higgs field H are localized in space (decaying for $|x| \to \infty$) and are oscillating in time; thus, they correspond to *oscillons* (alias breathers). At the leading-order in ε, the oscillation frequencies for A and H are given by: $\omega_A \approx 1$ and $\omega_H \approx 2$ (in units of m_A) respectively.

On the other hand, for $1.63 < q < 2$, we obtain $s < 0$ [repulsive (defocusing) nonlinearity], so that Eq. (2.16) possesses a kink solution of the following form:

$$u = u_0 \tanh\left(\sqrt{|s|} u_0 x_1\right) e^{-i\omega t_2}, \tag{2.21}$$

where u_0 is a $\mathcal{O}(1)$ free parameter and $\omega = u_0^2 |s|$. In this case, the approximate solutions for the gauge and Higgs fields read:

$$A \approx 2\varepsilon u_0 \tanh\left(\sqrt{|s|} \varepsilon u_0 x\right) \cos\left[\left(1 + (\varepsilon u_0)^2 |s|\right) t\right], \tag{2.22}$$

$$H \approx (\varepsilon u_0)^2 B \tanh^2\left(\sqrt{|s|} \varepsilon u_0 x\right) \left\{b + 2\cos\left[2\left(1 + \varepsilon^2 u_0^2 |s|\right) t\right]\right\}. \tag{2.23}$$

These solutions correspond to oscillating kinks, for both fields, which are zero exactly at the core of the kink and acquire non vanishing values at $|x| \to \infty$. Again the fields oscillate with the frequencies $\omega_A \approx 1$ and $\omega_H \approx 2$.

3. Numerical results

To further elaborate on our analytical findings, in this Section we will present results stemming from numerical integration of Eqs. (2.4)-(2.5). Our aim is to check the validity of our analytical predictions, namely the existence of oscillons and oscillating kinks, as well as study numerically their stability. The equations of motion are integrated by using a fourth-order Runge-Kutta time integrator and a pseudo-spectral method for the space derivatives [40]. The lattice spacing used was fixed to $\Delta x = 0.2$, the time step $\Delta t = 10^{-2}$, and the total length of the lattice $L = 400$. In all simulations we used, as an initial condition, the approximate solutions of Eqs. (2.19)-(2.20) for the oscillons and of Eqs. (2.22)-(2.23) for the oscillating kinks for $t = 0$; in all cases we have fixed the free parameter value to $u_0 = 1$, and the ratio of the two fields amplitudes to $\varepsilon = 0.1$.

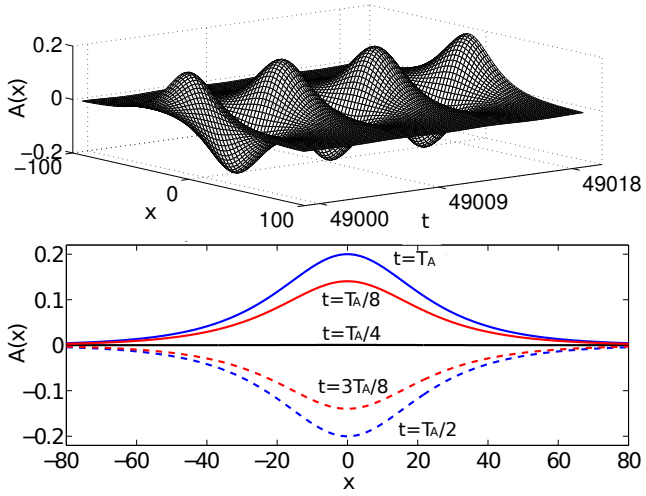

Figure 1: (Color online) Top panel: Evolution of the gauge field A as a function of x and t. Bottom panel: Profile snapshots of the field at different instants of its breathing motion. Parameter values used are $\varepsilon = 0.1$, $q = 1.5$ and the oscillation period is $T_A = 2\pi$.

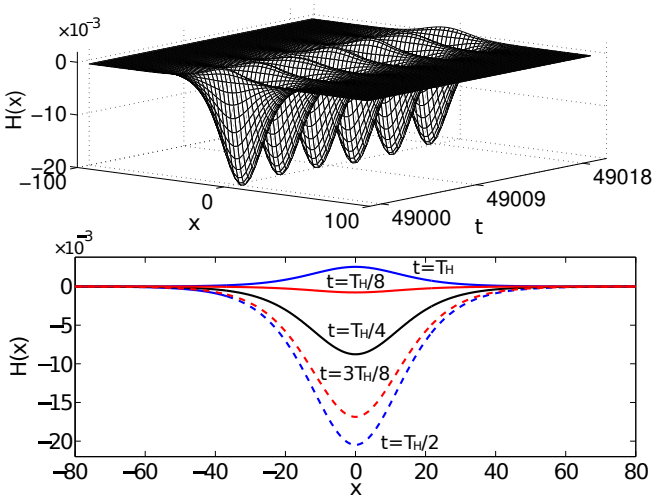

Figure 2: (Color online) Same as in Fig. 1, but for the Higgs field H. Notice that the oscilation period of the Higgs field is $T_H = \pi$.

3.1 Oscillons

In the top panels of Fig. 1 and Fig. 2 a contour plot showing the evolution of an oscillon solution is shown (for $q = 1.5$) at the end of the integration time $t = 5 \times 10^4$. Note that the periods of the two fields are $T_A \equiv 2\pi/\omega_A = 2\pi$ and $T_H \equiv 2\pi/\omega_H = \pi$, and thus 3 oscillations for the gauge field and 6 oscillations for the H field are depicted. In the bottom panels of Figs. 1 and 2, we show the profiles of A and H , during the interval of one period of exhibiting their breathing motion. While the gauge field A performs symmetric oscillations, the Higgs field oscillates asymmetrically with respect to its equilibrium point. This is due to the constant b in the solution of Eq. (2.20). The evolution of an oscillon for $q = 2.5$ (lying in the second region where oscillons exist) is also shown

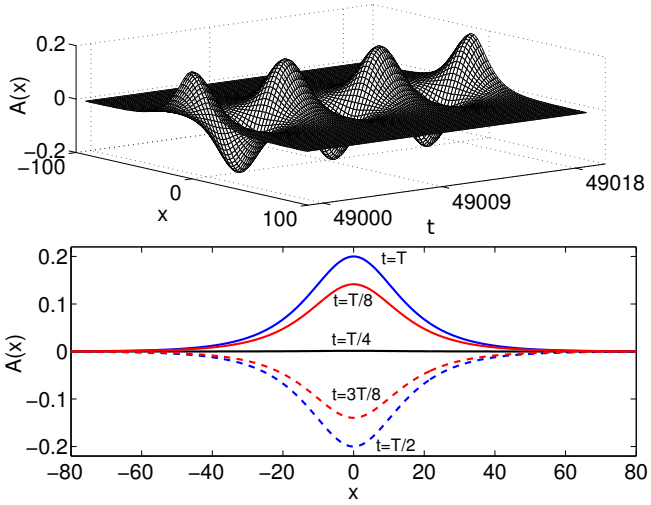

Figure 3: (Color online) Same as Fig. 1, for parameter values $\varepsilon = 0.1$ and $q = 2.5$.

in the top panels of Fig. 3 and Fig. 4. The breathers become more localized in this region, as can be seen from their snapshots (bottom panels of Figs. 3-4).

In order to demonstrate the localization of the energy of the oscillons, in the top and middle panels of Fig. 5, we show a contour of the total Hamiltonian density [cf. Eq. (2.6)] for $q = 1.5$. The top panel, corresponds to an initial condition using only Eqs. (2.19)-(2.20), while in the middle panel we have also added a random Gaussian noise to the initial condition, as large as 10% of the oscillon's amplitude (the rest of the parameters are as in Fig. 1). We observe that the energy density remains localized during the numerical integration in both cases (with and without noise). We would like to stress here that, the latter result, shows that oscillons are robust under the effect of a random noise, and this was also confirmed for different values of q in the domain of existence of the oscillon. For completeness, the total energy $E(t) = \int_{-\infty}^{\infty} \mathscr{H} dx$, normalized to its initial value $E(0)$, is also shown (dashed dotted line)in the bottom panel of Fig. 5. In fact the energy fluctuations, defined as $\Delta E = E - E(0)$, as shown in Fig. 5 [for $q = 1.5$ (top solid line) and $q = 2.5$ (bottom dashed line)] are of the order of 10^{-4}.

3.2 Spontaneous oscillon formation

In this section we show that oscillons can *emerge spontaneously*, through the mechanism of modulation instability (for more details see Ref. [41]). The latter concerns the instability of plane wave solutions of the NLS Eq. (2.16), of the form

$$u(x_1,t_2) = u_0 \exp\left[i\left(kx_1 - \omega t_2\right)\right], \tag{3.1}$$

under small perturbations. To briefly describe the emergence of this instability, we consider the following ansatz:

$$u = \left(u_0 + W\right) \exp\left[i\left(kx_1 - \omega t_2\right) + i\Theta\right)\right], \tag{3.2}$$

where the amplitude and phase perturbations W and Θ are given by:

$$W = \varepsilon W_0 \exp\left[i\left(Qx_1 - Pt_2\right)\right] + \text{c.c.}, \tag{3.3}$$

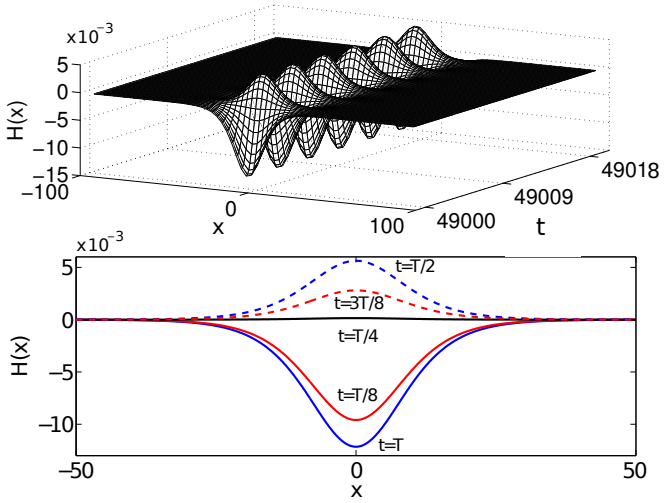

Figure 4: (Color online) Same as Fig. 2, with parameter values $\varepsilon = 0.1$, $q = 2.5$.

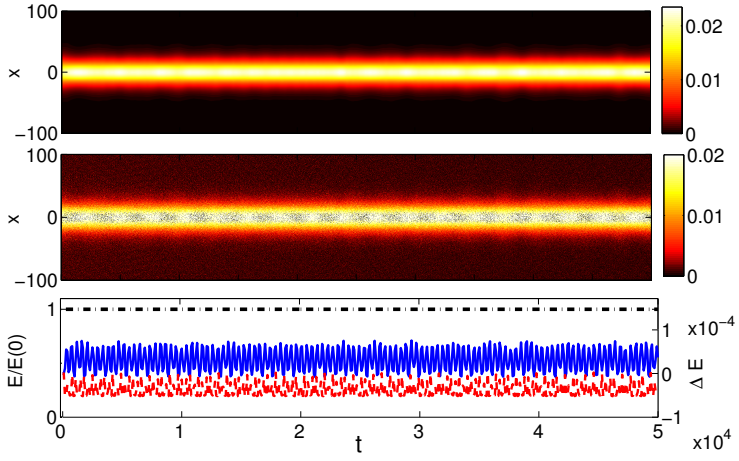

Figure 5: (Color online) Top and middle panel: contour plot showing the energy density $\mathscr{H}(t)$, as a function of time, for $q = 1.5$. For the middle panel the initial condition was perturbed by a small random noise with an amplitude 10% of the oscillon's amplitude. Bottom panel: the total energy normalized to its initial value at $t = 0$ dashed dotted line [upper (black)] . The energy difference ΔE, for $q = 1.5$ solid [middle (blue)] line and $q = 2.5$ dashed [bottom (red)] line.

$$\Theta = \varepsilon \Theta_0 \exp\left[i\left(Qx_1 - Pt_2\right)\right] + \text{c.c.}, \tag{3.4}$$

with W_0 and Θ_0 being constants, and ε being a formal small parameter. Substituting Eqs. (3.2)-(3.4) into Eq. (2.16) it is found that, for $k = 0$, the frequency P and the wavenumber Q of the perturbations, obey the dispersion relation:

$$P^2 = (1/2)|Q|^2(|Q|^2/2 - 2s|u_0|^2). \tag{3.5}$$

It is evident from Eq. (3.5) that for $s > 0$ there exists an instability band for wavenumbers $Q^2 < 4u_0^2 s$, where P becomes complex. Note that this instability can only emerge in the region where oscillons exist. When this instability manifests itself, the exponential growth of the perturbations leads to the

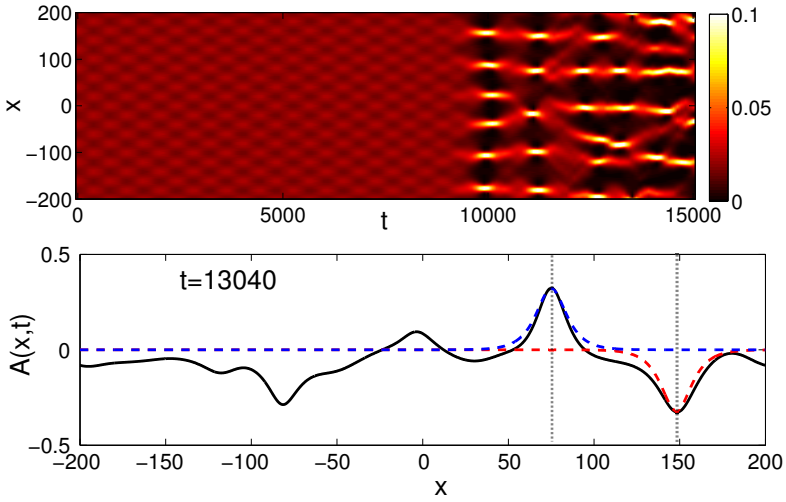

Figure 6: (Color online) Top panel: Contour plot showing the energy functional $\mathscr{H}(t)$, for $q = 1.5$, $Q = 0.1$, $u_0 = 1$, $\varepsilon = 0.1$ for an initial condition corresponding to an unstable plane wave. Bottom panel: Profile of the gauge field $A(x)$, (solid [black] line), at $t = 13040$ after the instability has set in. Dashed (blue and red) lines, correspond to the the solutions of Eq. (2.19), fitted with the parameter u_0 at the peak of the oscillons (indicated by the dotted [grey] lines at $x = 75$ and $x = 150$).

generation of localized excitations, which are identified as the oscillons described in Eqs. (2.19)-(2.20).

To illustrate the above, we have numerically integrated Eqs. (2.4)-(2.5), with an initial condition corresponding to the plane wave of Eq. (3.1), perturbed as in Eq. (3.2), with $\varepsilon = 0.1$, $W_0 = 1$, $Q = 0.1$ (inside the instability band), and $\Theta_0 = 0$; the rest of the parameters used are $q = 1.5$, $\varepsilon = 0.1$, $u_0 = 1$ and $k = 0$. In the top panel of Fig. 6, we show a contour plot of the energy density, $\mathscr{H}(t)$. It is observed that, at $t \sim 10,000$, localization of energy is observed due to the onset of the modulation instability. This localization is due to the fact that harmonics of the unstable wavenumber Q of the perturbation are generated, which deform the plane wave and lead to the formation of localized entities. In fact, the latter are eventually reformed into oscillons, as is clearly observed in the bottom panel of Fig. 6: there, we show the profile of the gauge field $A(x)$ [solid (black) line] at $t = 13040$, and we identify at least two well formed oscillons located at $x = 75$ and $x = 150$. The latter are found to be in a very good agreement with the analytical profile depicted by the dashed (red and blue) lines. To perform the fitting, we plotted the approximate solutions of Eq. (2.19), using the value at the peak of the oscillons, in order to identify the oscillon amplitude u_0. Then, the solution was also displaced by a constant factor, in order to match the center of the oscillon. Additionally, time was set to zero ($t = 0$) and the fitting was made at the beginning of the period of oscillation for the particular oscillons. The very good agreement between the analytical and numerical field profiles highlights the fact that the oscillons considered in this section can be generated spontaneously via the modulational instability mechanism.

3.3 Oscillating kinks

We now proceed with the numerical study of solutions corresponding to the kinks of the NLS Eq. (2.16). Such solutions in the form of Eqs. (2.22)-(2.23) are expected to exist in the parameter

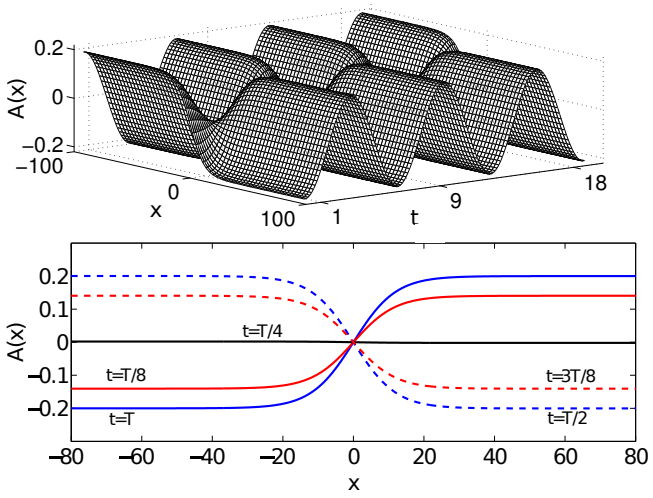

Figure 7: (Color online) Same as Fig. 1, but for a kink solution, for $q = 1.8$.

region $1.63 < q < 2$. Performing the same procedure as in the previous section, we numerically integrate the equations of motion and study the relevant dynamics. In the top panels of Figs. 7 and 8, the contour plot of a kink solution is plotted, showing the evolution of both fields A and H, during the interval of three and six periods, respectively (for $q = 1.8$). In addition, the profiles of both fields are shown in the bottom panels of Figs. 7- 8. The oscillating kinks were found to be unstable for all values of the parameter q within their region of existence. The instability is manifested by an abrupt deformation of the kink solution, even near its core, characterized by the inverse width l_d, (where $l_d = 2\sqrt{|s|}\varepsilon u_0$). In Fig. 9, the top panel shows the profiles of the gauge field at the beginning ($t = 8$) [solid (blue) line], and at the end of the integration ($t = 1200$) [solid (red) line]. While the shape of the kink is more or less preserved, it is clear that the solution profile has been significantly deformed. More importantly, the Higgs field H, shown in the bottom panel, not only has been distorted but it has also become an order of magnitude larger than its initial amplitude. Thus, it can be concluded that oscillating kinks are unstable.

4. Discussion and conclusions

In this work we have presented a class of classical solutions of the 1D Abelian Higgs model obtained with the use of a multiscale expansion method. The key assumption in our treatment is that the scalar field amplitude is much smaller than that of the gauge field; the relevant ratio was then used as a formal small parameter in the perturbation expansion. We have shown that the equations of motion can be reduced to a NLS equation; by means of the latter, localized solutions in the form of oscillons and oscillating kinks were derived. Results by numerical integration of the original equations of motion where found to be in very good agreement with the analytical findings. In addition, we have numerically studied stability of the solutions against a Gaussian noise with amplitude up to 10% of the Higgs field amplitude, and found that the oscillons remain robust. The robustness of oscillons is also complemented by more recent findings [34] where it is indicated that only oscillon solutions for the gauge and the Higgs field are long-lived. This leads us to the conclusion that oscillons dominate in the solution space of the Abelian-Higgs model.

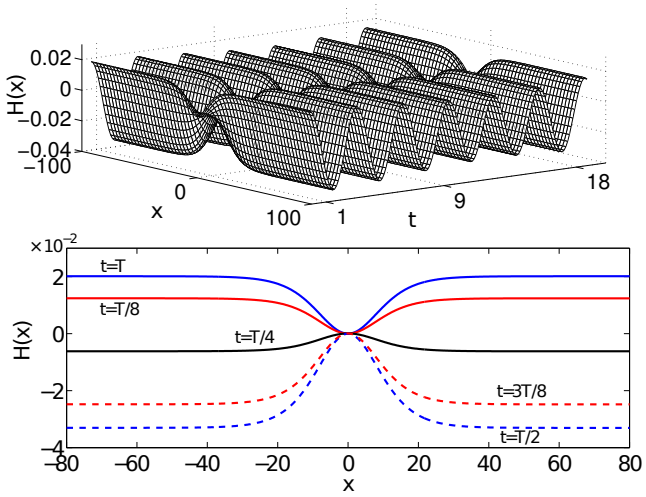

Figure 8: (Color online) Same as Fig. 2 for the kink solution, and for $q = 1.8$.

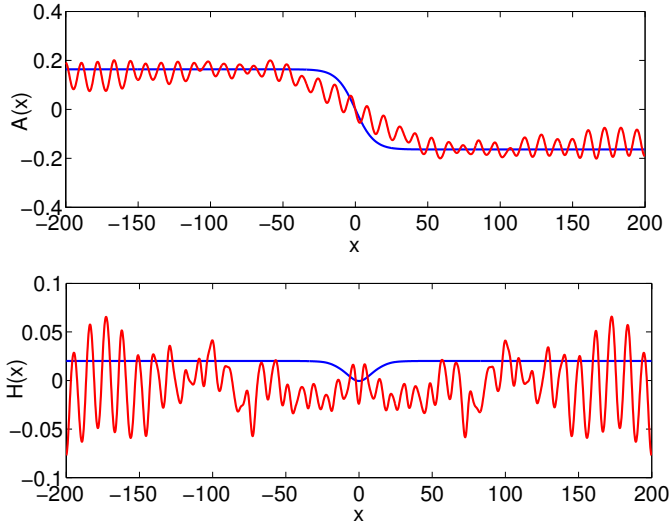

Figure 9: (Color online) Top panel: profile snapshots of the gauge field at the beginning [solid (blue) line], and at the end of the simulation [solid (red) line], for $q = 1.8$. Bottom panel: same as in top panel but for the Higgs field.

It is also relevant to discuss the possible connection of the presented solutions to the physics of superconductors. One could, in principle, write down the form of the magnetic and electric fields originating from the gauge field A which was chosen to be in the $\hat{y}$ direction: $\vec{B}(x,t) = \partial_x A(x,t)\hat{z}$, and $\vec{\mathscr{E}}(x,t) = -\partial_t A(x,t)\hat{y}$.

In the case of the oscillon solutions given in Eqs. (2.19)-(2.20), the above equations describe the electric field in the y direction, which produces a magnetic field in the z direction; both fields are localized around the origin of the x axis – cf. Fig. 10, where the profiles of the fields are shown. This can be thought of as a configuration, describing Superconductor–Normal metal–Superconductor (SNS) Josephson junction [37], where two superconductors are linked by a thin normal conductor

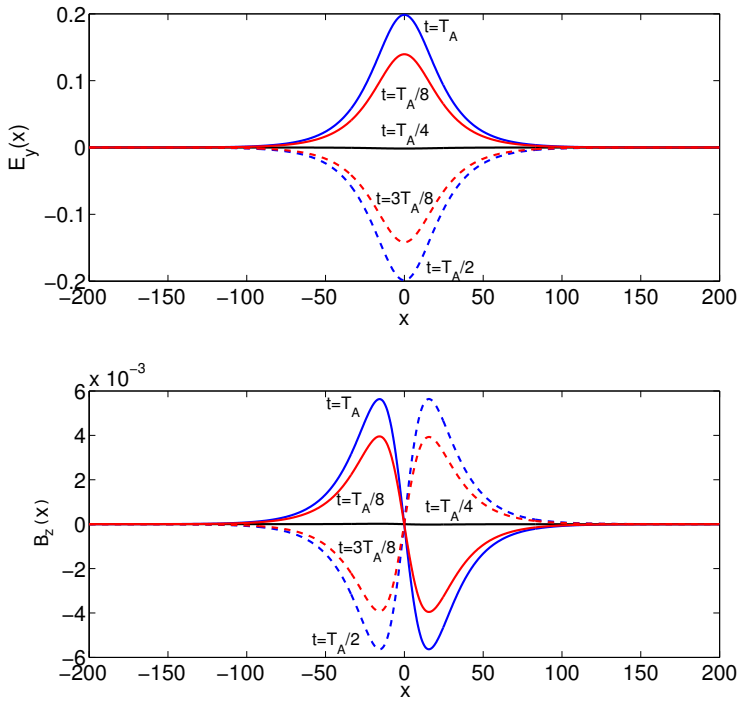

Figure 10: (Color online) Top panel: profile snapshots of the electric field $\mathscr{E}_y(x)$ for $q = 1.5$. Bottom panel: profile snapshots of the magnetic field $B_z(x)$ for the same q.

placed at the origin. Then, our solutions describe a condensate $\phi = (\upsilon + H(x,t))/\sqrt{2}$ that oscillates around its vev near the origin, and acquires its vev value when entering the superconductors. Accordingly, the magnetic field is shown to oscillate inside the normal conductor, but vanishes exponentially inside the superconductors as per the Meissner effect.

Our approach not only reveals a new class of solutions of the Abelian-Higgs model, but also dictates a straightforward general strategy for the search of non-trivial dynamics in models involving classical fields with nonlinear interactions. In particular the dynamics of such models is governed by the nonlinear Schrödinger equation. It is an interesting perspective to determine the impact of these solutions on the thermal and quantum behaviour of the involved fields. Such studies is an interesting theme for future work.

Acknowledgments. Illuminating discussions with L. P. Gork'ov are kindly acknowledged.

References

[1] E. J. Weinberg, *Classical Solutions in Quantum Field Theory* (Cambridge University Press, Cambridge, England, 2012). M. Gleiser, Int. J. Mod. Phys. D **16**, 219 (2007); A. Rajantie, and E. J. Copeland, Phys. Rev. Lett. **85**, 916 (2000).

[2] M. A. Amin, R. Easther, H. Finkel, R. Flauger, and M. P. Hertzberg, Phys. Rev. Lett. **108**, 241302 (2012).

[3] N. Graham, N. Stamatopoulos, Phys. Lett. B **639**, 541 (2006);E. Farhi, N. Graham, A. H. Guth, N. Iqbal, R. R. Rosales, and N. Stamatopoulos, Phys. Rev. D **77**, 085019 (2008).

[4] S. Coleman, *Aspects of Symmetry* (Cambridge University Press, Cambridge, England, 1985); R. Rajaraman, *Solitons and Instantons* (North-Holland, Amsterdam, 1982).

[5] P. B. Umbanhowar, F. Melo, and H. L. Swinney, Nature **382**, 793 (1996); L. S. Tsimring and I. S. Aranson, Phys. Rev. Lett. **79**, 213 (1997).

[6] J. Rajchenbach, A. Leroux, and D. Clamond, Phys. Rev. Lett. **107**, 024502 (2011); H. Xia, T. Maimbourg, H. Punzmann, and M. Shats, Phys. Rev. Lett. **109**, 114502 (2012);

[7] R. F. Dashen, B. Hasslacher, and A. Neveu, Phys. Rev. D**11**, 3424 (1975); B. Piette, and W. J. Zakrzewski, Nonlinearity **11**, 1103 (1998).

[8] I.L. Bogolyubskii, and V.G. Makhan'kov, [JETP Lett. **24**, 12 (1976)]; I.L. Bogolyubskii, and V.G. Makhan'kov, JETP Lett. **25**, 107 (1977).

[9] D. K. Campbell, J. F. Schonfeld, and C. A. Wingate, Physica, D **9**, 1 (1983).

[10] M. Gleiser, Phys. Rev. D **49**, 2978 (1994); E. J. Copeland, M. Gleiser, H. -R. Müller, Phys. Rev. D **52**, 1920 (1995); M. Gleiser, R. M. Haas, Phys. Rev. D **54**, 1626 (1996).

[11] E. P. Honda, and M. W. Choptuik, Phys. Rev. D **65**, 084037 (2002).

[12] M. Hindmarsh, and P. Salmi, Phys. Rev. D **74**, 105005 (2006).

[13] M. Hindmarsh, and P. Salmi, Phys. Rev. D **77**, 105025 (2008).

[14] G. Fodor, P. Forgács, P. Grandclément, and I. Rácz, Phys. Rev. D **74**, 124003 (2006).

[15] G. Fodor, P. Forgács, Z. Horváth, and Á. Lukács, Phys. Rev. D **78**, 025003 (2008).

[16] M. Gleiser, and D. Sicilia, Phys. Rev. Lett. **101**, 011602 (2008).

[17] H. Segur, and M. D. Kruskal, Phys. Rev. Lett. **58**, 747 (1987).

[18] M. Gleiser and J. Thorarinson, Phys. Rev. D **76**, 041701(R) (2007);M. Gleiser and J. Thorarinson, Phys. Rev. D **79**, 025016 (2009).

[19] E. Farhi, N. Graham, V. Khemani, R. Markov, and R. Rosales, Phys. Rev. D **72**, 101701(R) (2005).

[20] N. Graham, Phys. Rev. Lett. **98**, 101801 (2007); N. Graham, Phys. Rev. D **76**, 085017 (2007).

[21] E. I. Sfakianakis, arXiv:hep-th/1210.7568.

[22] L. P. Pitaevskii, and S. Stringari, *Bose-Einstein Condensation* (Oxford University Press, Oxford, 2003).

[23] Y.-J. Lin, K. Jimenez-Garcia, and I. B. Spielman, Nature **471**, 83 (2011).

[24] L. J. Garay, J. R. Anglin, J. I. Cirac, and P. Zoller, Phys. Rev. Lett. **85**, 4643 (2000).

[25] P. G. Kevrekidis, D. J. Frantzeskakis and R. Carretero-González (eds.), *Emergent Nonlinear Phenomena in Bose-Einstein Condensates: Theory and Experiment* (Springer-Verlag, Heidelberg, 2008).

[26] L. P. Gork'ov, Sov. Phys. JETP **36**, 1364 (1959).

[27] L. P. Gork'ov and G. M. Eliashberg, Z. ÃL'ksp. Teor. Fiz. **54**, 612 (1968) [Sov. Phys. JETP **27**, 328 (1968)]

[28] V. L. Ginzburg, L.D. Landau, Zh. Eksp. Teor. Fiz. **20**, 1064 (1950).

[29] A. A. Abrikosov, Zh. Eksp. Teor. Fiz. **32**, 1442 (1957) [Sov. Phys. JETP **5**, 1174 (1957)].

[30] A. Vilenkin and E. P. S. Shellard, *Cosmic Strings and Other Topological Defects* (Cambridge University Press, Cambridge, England, 1994).

[31] L. D. Landau and E. M. Lifshitz *Statistical Physics* (Pergamon, New York, 1980), 3rd ed., part 2.

[32] C. Rebbi and R. Singleton, Jr., Phys. Rev. D **54**, 1020 (1996); P. Arnold and L. McLerran, Phys. Rev. D **37**, 1020 (1988).

[33] V. Achilleos, F. K. Diakonos, D. J. Frantzeskakis, G. C. Katsimiga, X. N. Maintas, E. Manousakis, C. E. Tsagkarakis, and A. Tsapalis, Phys. Rev. D **88**, 045015 (2013).

[34] F. K. Diakonos, G. C. Katsimiga, X. N. Maintas, and C. E. Tsagkarakis, Phys. Rev. E **91**, 023202 (2015).

[35] A. Jeffrey and T. Kawahara, *Asymptotic methods in nonlinear wave theory*, Pitman (1982).

[36] X. N. Maintas, C. E. Tsagkarakis, F. K. Diakonos, and D. J. Frantzeskakis, J. Mod. Phys. **3**, 637 (2012), arXiv:1306.6765v1; V. Achilleos, F. K. Diakonos, D. J. Frantzeskakis, G. C. Katsimiga, X. N. Maintas, C. E. Tsagkarakis, and A. Tsapalis, Phys. Rev. D **85**, 027702 (2012).

[37] A. Barone and G. Paterno, *Physics and Applications of the Josephson Effect* (Wiley-Interscience, New York, 1982).

[38] Yu. S. Kivshar and G. P. Agrawal, *Optical solitons: from fibers to photonic crystals* (Academic Press, San Diego, 2003).

[39] R. S. Johnson, *A modern introduction to the mathematical theory of water waves* (Cambridge University Press, Cambridge, 2005).

[40] J. Yang, *Nonlinear Waves in Integrable and Nonintegrable Systems* (SIAM, Philadelphia, USA, 2010).

[41] The destabilization of plane waves under small-amplitude long-wavelength perturbations is known as modulational instability or Benjamin-Feir instability [T. B. Benjamin and J. E. Feir, J. Fluid Mech. **27**, 417 (1967)], and occurs in various contexts, including fluid mechanics [G. B. Whitham, J. Fluid Mech. **22**, 273 (1965)], dielectrics [L. A. Ostrovsky, Sov. Phys. JETP **24**, 797 (1967)], plasmas [A. Hasegawa, Phys. Fluids **15**, 870 (1972)], etc.